Noyes, R. M. (1956) *J. Am. Chem. Soc. 78*, 5486-5490.
Noyes, R. M. (1961) *Prog. React. Kinet. 1*, 131-160.
Reynolds, A. H., Rand, S. D., & Rentzepis, P. M. (1981) *Proc. Natl. Acad. Sci. U.S.A. 78*, 2292-2296.
Stetzkowski, F., Banerjee, R., Marden, M. C., Beece, D. K., Bowne, S. F., Doster, W., Eisenstein, L., Frauenfelder, H., Reinisch, L., Shyamsunder, E., & Jung, C. (1985) *J. Biol. Chem. 260*, 8803-8809.

A Raman Spectroscopic Study of Hen Egg Yolk Phosvitin: Structures in Solution and in the Solid State†

B. Prescott,‡ V. Renugopalakrishnan,§ M. J. Glimcher,§ A. Bhushan,‡ and G. J. Thomas, Jr.*,‡

Department of Chemistry, Southeastern Massachusetts University, North Dartmouth, Massachusetts 02747, and Laboratory for the Study of Skeletal Disorders and Rehabilitation, Department of Orthopedic Surgery, Harvard Medical School, Children's Hospital, Boston, Massachusetts 02115

Received November 4, 1985; Revised Manuscript Received January 14, 1986

ABSTRACT: Laser Raman spectroscopy has been employed to study the structure of the hen egg yolk protein phosvitin in H_2O and D_2O solutions at neutral and acidic pH (pD) and in the solid state. The Raman data indicate an unusual conformation for phosvitin in neutral aqueous solution, which is deficient in both α-helix and conventional β-sheet conformations. This unusual pH 7 structure is, however, largely converted to a β-sheet conformation in strongly acidic media (pH <2). β-Sheet is also the predominant secondary structure for phosvitin in the solid state, obtained by lyophilization of the protein from aqueous solution at neutral pH. The imidazolium rings of histidyl residues remain significantly protonated near neutrality, which suggests substantial elevation of the pK for imidazolium ring ionizations of phosvitin in aqueous solution. This may result from extensive ion-pair interactions involving positively charged histidines and negatively charged phosphoserines, which are prevalent in the phosvitin sequence. The present results suggest that antiparallel β-sheets may not be the secondary structure most characteristic of native phosvitin (physiological pH), even though β-sheet is the predominant conformation for phosvitin in acidic solutions (pH 1.5) and in the lyophilized solid. Phosvitin appears to be the first protein for which the major component to the Raman amide I band is centered near 1685 cm^{-1}, which is 10-40 cm^{-1} higher than proteins heretofore examined in aqueous solution by Raman spectroscopy.

Phosvitin, a phosphoglycoprotein of M_r 34 000, is the major protein component of hen egg yolk. The carbohydrate moiety, covalently linked to an asparagine residue, accounts for only about 6.5% of the molecular mass (Shainkin & Perlmann, 1971). The phosvitin sequence of 216 residues is known and exhibits many unusual features, including 123 serines (S),[1] virtually all of which are phosphorylated, 15 lysines (K), 13 histidines (H), and 11 arginines (R) (Byrne et al., 1984). The three-dimensional structure of phosvitin has not yet been determined, and the relevance of the high density of charged side chains to phosvitin function as a transport protein is not known. Accordingly, considerable interest has been focused on the secondary structure of the phosvitin polypeptide chain.

Previous spectroscopic studies suggest several different possibilities for the conformation of the protein chain at physiological pH. Infrared data from D_2O solutions of phosvitin have been interpreted as indicative of an α-helix structure near neutrality (Timasheff et al., 1967). Circular dichroism (CD) investigations, on the other hand, have indicated an irregular structure near neutral pH and a β-sheet structure at acidic pH (Taborsky, 1970; Perlmann & Grizzuti, 1971). NMR results are consistent with an open and flexible structure near pH 7, in which most serine phosphate dianions are accessible to solvent but many of the histidines are not (Vogel, 1983). Recent investigations using CD and Fourier transform infrared (FTIR) spectroscopy have suggested substantial β-sheet conformation in both the solid and solution phases. A secondary structure model has been proposed on the basis of the FTIR spectroscopic results and a secondary structure prediction algorithm (Renugopalakrisnan et al., 1985).

We have undertaken an investigation of the Raman spectrum of phosvitin in the expectation that the Raman data would help to resolve apparent inconsistencies in the previously reported secondary structures. An advantage of Raman spectroscopy is the capability of comparing structural information from both normal and deuterated forms of the protein in solid and solution states. Since interference from liquid water is scant and easily compensated in Raman spectra, the structure-sensitive Raman bands of the protein are easily and reliably compared as a function of the solution pH. The Raman spectrum is also rich in frequencies that originate from vibrations of the amino acid side chains. This property can be exploited to obtain information about the ionization states of phosphoserines and histidines of phosvitin. Interpretation of the conformation-sensitive Raman amide I bands of phosvitin is facilitated by the use of digital methods for both

†Supported by NIH Grants AI11855 (G.J.T.) and AM34078 (M.J.G.) and by the Peabody Home for Crippled Children, Inc.
*Author to whom correspondence should be addressed.
‡Southeastern Massachusetts University.
§Children's Hospital.

[1] Abbreviations: Generally, one-letter symbols are employed for the amino acids. The abbreviation S is used for both serine and phosphoserine. The structure to which it applies is clear from the context in which it is used.

0006-2960/86/0425-2792$01.50/0

enhancement of spectral resolution (Fourier deconvolution) and quantitative analysis of the band profile (curve fitting).

Experimental Procedures

Materials. Phosvitin was isolated from chicken eggs according to the method of Joubert and Cook (1958) and was resolved into two phosphoprotein components on a Sephadex G-100 column (Clark, 1970). The samples used for Raman spectroscopy were from the major fraction collected by this procedure. The amino acid composition (mol %) of this fraction is 3.36 A, 7.14 D, 5.08 E, 0.48 F, 2.37 G, 5.67 H, 0.88 I, 7.35 K, 1.38 L, 0.25 M, 1.49 P, 5.18 R, 55.42 S, 1.91 T, 1.39 V, 0.59 W, and 0.06 Y.

Mannose, galactose, *N*-acetylglucosamine, sialic acid, poly(L-serine), and phosphoserine were obtained from Sigma Chemical and were used without further purification. Deuterium oxide (99.8% D_2O), deuterium chloride (DCl), and sodium deuterioxide (NaOD) were obtained from Aldrich Chemical or Bio-Rad.

Methods. Solutions of phosvitin were prepared by dissolving the protein to a concentration of approximately 100 mg/mL in the appropriate solvent depending on the pH (or pD) value desired. For neutral solutions, the pH (pD) was maintained at 7.4 ± 0.3 by the addition of either HCl (DCl) or NaOH (NaOD), as required. For acidic solutions, the pH (pD) was adjusted similarly to a value of 1.5 ± 0.3.

pH (pD) was measured with a microelectrode. The solutions were transferred to glass capillary cells, which were then sealed at both ends. Solutions of poly(L-serine) and phosphoserine were prepared similarly. Solid samples were suspended in H_2O (D_2O) at the indicated pH (pD) values.

Raman spectra were excited with approximately 300 mW of the 514.5-nm line of an argon ion laser (Spectra Physics Model 171-18) and were recorded on a Spex Ramalog V/VI spectrometer, operating under the control of a North Star Horizon II microcomputer (Li et al., 1981). Spectral data were recorded with a slit width of 8 cm^{-1} at increments of 1 cm^{-1} and with an integration time of 1 s. Each spectrum displayed is the average of eight or more scans and has been corrected for background fluorescence and solvent interference. All spectra were reversible with respect to increases or decreases in pH and pD. Further details of the sample handling required for Raman spectroscopy have been described previously (Verduin et al., 1984).

For Fourier deconvolutions of the amide I region (1500–1750 cm^{-1}), a Gaussian–Lorentzian product function of 25-cm^{-1} half-width was chosen as the desmearing function. Deconvolution was performed on either a VAX 11/780 or an IBM personal computer, the latter with an Intel 8087 numeric data processor installed. Further discussions of the deconvolution method, including its advantages, limitations, and application to Raman spectra of proteins, have been given elsewhere (Thomas & Agard, 1984; Thomas, 1985).

For curve fitting of the amide I profile, we used the protein reference data set and programs of Dr. Robert W. Williams, who generously provided assistance in the implementation of his method (Williams, 1983). The Williams' programs were adapted to run on a DEC-20 computer, on which all of the present curve fitting computations were carried out.

Results and Discussion

Raman Spectrum of Phosvitin Is Dominated by Bands from the Protein Backbone and Phosphoserine Side Chains. The Raman spectra of phosvitin in aqueous solutions at pH 7.4 and 1.5 are shown in Figure 1. Corresponding D_2O solution spectra are presented in Figure 2. Included in Figure 1 is

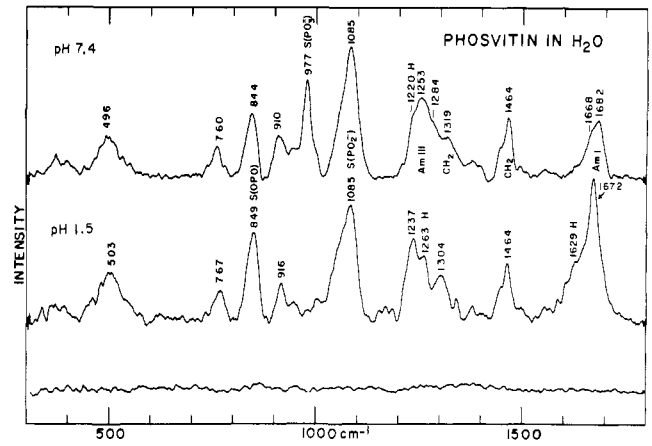

FIGURE 1: Raman spectra of H_2O solutions of phosvitin (100 mg/mL) in the region 300–1800 cm^{-1} at pH 7.4 (top) and 1.5 (middle). The bottom spectrum was obtained from a mixture of mannose (1.5 mg/mL), galactose (1.58 mg/mL), sialic acid (1.85 mg/mL), and *N*-acetylglucosamine (2.98 mg/mL), which corresponds to the carbohydrate composition of phosvitin in the top and middle spectra. Labels indicate Raman frequencies in cm^{-1} and assignments based upon model compound analyses (Table I). Each spectrum is the average of eight scans and has been corrected for the background and solvent scattering.

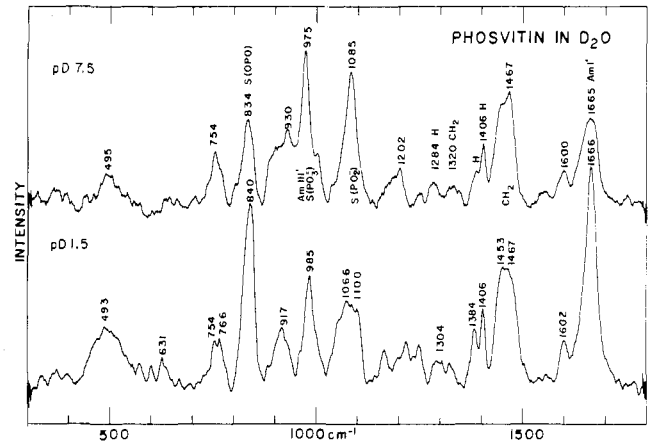

FIGURE 2: Raman spectra of D_2O solutions of phosvitin (100 mg/mL) in the region 300–1800 cm^{-1} at pD 7.5 (top) and 1.5 (bottom). Labels and other conditions are as given in Figure 1.

the spectrum of a mixture of sugars that matches the carbohydrate composition of phosvitin. The absence of any strong bands in the spectrum of the sugar mixture indicates that the carbohydrate moiety of the phosphoglycoprotein is virtually Raman transparent when compared with its protein and phosphoserine constituents.

The spectra of phosvitin (Figures 1 and 2) clearly differ greatly from spectra of other proteins, a consequence of both the high content of serine residues and their phosphorylation. In order to assign the serine bands, we have obtained Raman spectra of the model compounds poly(L-serine) (Figure 3) and phosphoserine (not shown). For the assignment of phosphate bands, we have also referred to the well-known Raman spectral characteristics of mononucleotides (Lord & Thomas, 1967), the phosphate bands of which are identical with those of other monoesters of the orthophosphate group, including phosphoserine. Straightforward comparison of the model compound data with Figure 1 and 2 permits assignment of most of the Raman lines in the phosvitin spectra as indicated in Table I. Many of the assignments are also labeled in Figures 1 and 2.

In Figure 3 we note the intense and sharp amide I (1671) and amide III (1231-cm^{-1}) bands of the poly(L-serine) suspension in H_2O, indicative of an antiparallel β-pleated sheet

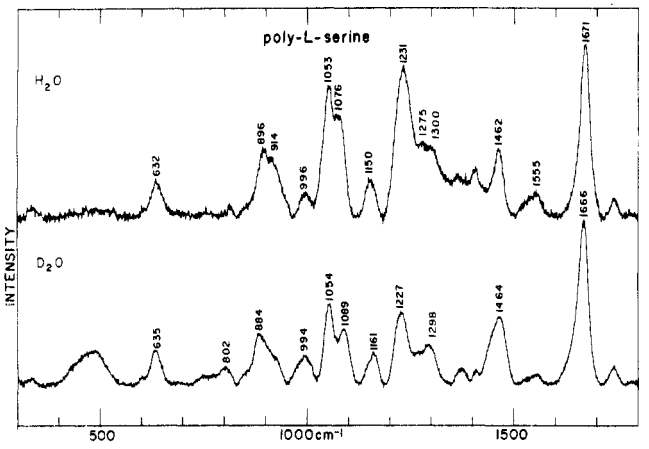

FIGURE 3: Raman spectra of poly(L-serine) in the region 300–1800 cm^{-1}: (top) solid suspension in H_2O; (bottom) deuterated solid suspension in D_2O.

Table I: Raman Frequencies and Assignments of Phosvitin[a]

solid	pH 7.4 soln	pH 1.5 soln	assignment	
			residue	mode
488 (8)	496 (7)	503 (9)	S	
767 (3)	760 (5)	767 (5)	S, W	
844 (4)	844 (10)	849 (13)	S	OPO stretch
912 (4)	910 (7)	916 (6)		CC stretch
946 (sh)	945 (5)	947 (2)		CH_3 rock
978 (8)	977 (16)		S	PO_3^{2-} stretch
	1004 (sh)	1003 (3)	F	ring
1071 (9)	1070 (sh)	1070 (sh)	S	CO stretch
1092 (9)	1085 (20)	1085 (20)	S	PO_2^- stretch
1163 (1)		1178 (2)		CH_3 rock
	1220 (sh)		H	ring
1243 (11)		1237 (14)	backbone	amide III (sheet)
	1253 (13)		backbone	amide III (unknown)
1261 (sh)	1260 (sh?)	1263 (12)	H	ring, protonated
	1284 (sh)		backbone	amide III (helix)
1313 (8)	1319 (7)	1304 (8)		CH_2 deformation
1337 (sh)		1341 (4)		CH_2 deformation
1376 (3)	1379 (3)	1379 (2)	W	ring
1406 (2)	1398 (2)		D, E	CO_2^- stretch
1446 (sh)	1447 (sh)	1447 (sh)		CH_3 deformation
1463 (10)	1464 (10)	1464 (10)		CH_2 deformation
	1494 (2)	1496 (2)	H	NH bending
1559 (2)	1554 (1)	1560 (2)	W	ring
1584 (1)		1586 (4)	H	ring
1633 (sh)	1629 (sh)	1629 (sh)	H	ring
1673 (14)	1668 (sh)	1672 (25)	backbone	amide I (sheet)
	1682 (9)		backbone	amide I (unknown)

[a] Abbreviations: sh = shoulder; H = histidine; S = phosphoserine; F = phenylalanine; W = tryptophan; D = aspartic acid; E = glutamic acid. Frequencies are accurate to ±3 cm^{-1}. Values in parentheses are relative peak heights normalized to 10.0 for the 1464-cm^{-1} band in each spectrum.

structure for this polypeptide. For the D_2O suspension, amide I′ is shifted as expected to lower frequency (1666 cm^{-1}). However, considerable intensity remains in the amide III region (ca. 1227 cm^{-1}), suggesting incomplete deuterium exchange of the polypeptide, which is not uncommon for β-sheet structures of this type (Williams et al., 1984). The amide III′ band of poly(L-serine) presumably occurs near 985 cm^{-1} and is observed as a low-frequency shoulder contributing to the broad band centered at 994 cm^{-1} for the D_2O suspension. Additional amide III′ intensity may also occur near 930 cm^{-1}. It is also evident from Figure 3 that the moderate Raman intensity near 1300 cm^{-1} is not deuteration sensitive and therefore is probably not associated with an amide III vibration. Raman bands near this frequency arise from conformation-sensitive side-chain methylene deformation modes and are present in most proteins (Thomas et al., 1983), including phosvitin (cf. Figures 1 and 2).

Peptide Backbone of Phosvitin Assumes an Unusual Structure in Neutral Aqueous Solutions. The amide I peak of phosvitin at 1682 cm^{-1} is unusually high in frequency. A discernible shoulder is also indicated at 1668 cm^{-1}. The amide III region of the spectrum contains a strong band at 1253 cm^{-1} with a weak shoulder at 1284 cm^{-1}. The additional shoulder near 1220 cm^{-1} is just outside the amide III region and can be assigned entirely to histidines (Ashikawa & Itoh, 1979). A contribution from protonated histidines is also expected near 1265 cm^{-1} and may contribute to the rather substantial breadth of the 1253-cm^{-1} amide III band.

The absence of intense amide III Raman scattering below 1245 cm^{-1} or above 1270 cm^{-1} and the absence of intense amide I scattering below 1680 cm^{-1} are both strong indications of deficiencies in ordered α-helical and β-sheet structures of conventional geometry in phosvitin (Chen & Lord, 1974). In fact, the observed amide I peak (1682 cm^{-1}) occurs at a frequency higher than that of any other protein heretofore examined. Although normal coordinate calculations (Krimm & Bandekar, 1980) and model compound studies (Seaton, 1983) of oligopeptides suggest that such a high-frequency Raman amide I mode could be characteristic of type I and type II β-turn structures, such an assignment is clearly inconsistent with the very intense amide III peak at 1253 cm^{-1}. For β-turns, both the calculations (Krimm & Bandekar, 1980) and the experimental data (Seaton, 1983; Lagant et al., 1984a,b) locate amide III in the interval 1290–1330 cm^{-1}. We observe a weak shoulder near 1319 cm^{-1} in phosvitin at pH 7.4 (Figure 1), but its presence also in the pD 7.5 spectrum (Figure 2) implicates the band in whole or n part as a methylene side-chain mode. Clearly, the intensity of a putative amide III component within the interval 1290–1330 cm^{-1} would be far too low to attribute its origin to the same structural feature that yields the intense 1682-cm^{-1} amide I band. Among known structures, only disordered or irregular chains are expected to yield Raman amide III in the vicinity of 1253 cm^{-1} (Chen & Lord, 1974). We conclude, therefore, that in neutral aqueous solution phosvitin does not contain a secondary structure dominated either by α-helix, β-sheet, or β-turn structures, or by any simple combination of them.

The predominant secondary structure of phosvitin at pH 7 that gives rise to the 1682-cm^{-1} amide I and 1253-cm^{-1} amide III peaks cannot be deduced from currently available Raman data on model compounds of known conformation. The inapplicability of extant models to phosvitin is not a consequence of the unusual side chains as such, since the phosphoserines and histidines do not contribute significantly to the Raman spectra in the regions of amide I and amide III bands. We believe the present data are indicative of an unusual secondary structure not encountered previously in either globular proteins or model polypeptides.

The above conclusion reached from H_2O solution spectra of phosvitin is supported also by the Raman data from D_2O solutions. An unusually broad amide I′ band near 1665 cm^{-1} is observed for phosvitin at pD 7.5 (Figure 2). Note, also, that the D_2O solution of the protein lacks residual amide III bands of appreciable intensity in the 1230–1280-cm^{-1} interval, indicating virtually complete deuterium exchange. [The weak band at 1284 cm^{-1} is due to histidine side chains (Harada et al., 1982).] Although a rigorous quantitative study of the rate of deuterium exchange was not made, we observed that the exchange was completed within the time frame of preparing the D_2O solution and recording its Raman spectrum (ca. 30 min). Phosvitin thus differs from many other proteins exam-

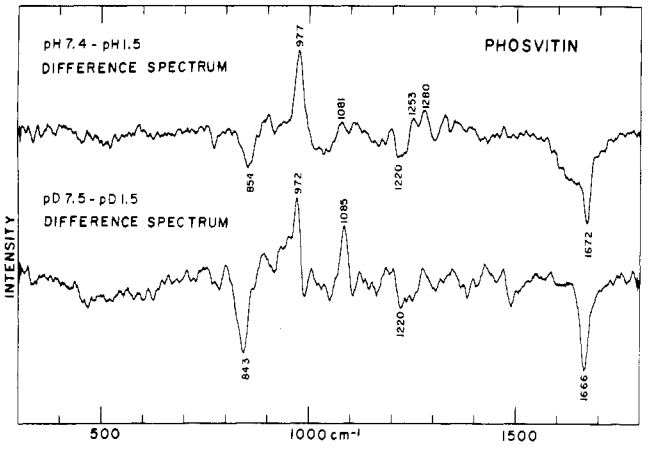

FIGURE 4: Raman difference spectra showing the pH-induced structure transition of phosvitin: (top) spectrum at pH 7.4 minus spectrum at pH 1.5; (bottom) spectrum at pD 7.5 minus spectrum at pD 1.5.

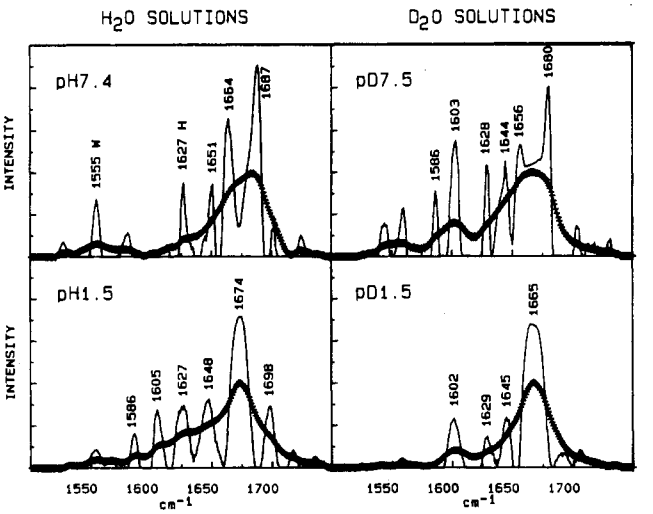

FIGURE 5: Fourier deconvolution of the Raman amide I and I′ bands of phosvitin: (left) amide I at pH 7.4 (top) and 1.5 (bottom); (right) amide I′ at pD 7.5 (top) and 1.5 (bottom). Labels indicate frequencies and assignments of the prominent bands. A Gaussian–Lorentzian deblurring function 25-cm^{-1} half-width was employed (Thomas, 1985). Other choices of the deblurring function alter the speed of convergence of the deconvolution algorithm but do not significantly affect the peak positions.

ined recently (Williams et al., 1984) and undergoes relatively rapid and complete deuterium exchange of amide NH groups. The Raman data, therefore, support the concept of an "open" or solvent-accessible structure in which D_2O molecules readily exchange with the entire protein backbone.

The amide III′ region (900–1000 cm^{-1}) of the spectrum of deuterated phosvitin, though potentially informative of the secondary structure, is partly obscured in neutral D_2O solution by the intense 975-cm^{-1} line of the phosphomonoester dianion of phosphoserine as shown in Figure 2 (see also below).

Phosvitin Undergoes a Large-Scale Conversion to β-Sheet Conformation in Acidic Media. The amide I and III bands of phosvitin at pH 1.5 differ greatly from those at neutral pH (Figure 1). Amide I is strong and sharp and is centered at 1672 cm^{-1}, which is characteristic of β-sheet structure. The intense amide III band at 1237 cm^{-1} is also characteristic of a high β-sheet content. [Again, we note that the 1263-cm^{-1} shoulder is assigned to protonated histidines and not to an amide III vibration (Ashikawa & Itoh, 1979).]

Similar indicators of β-sheet are evident in the Raman spectra of phosvitin at pD 1.5 (Figure 2), especially the strong amide III′ band at 985 cm^{-1} (Chen & Lord, 1974). The amide bands of the low-pH form of phosvitin are, in fact, very similar to the corresponding bands of the β-sheet structure of poly(L-serine) (Figure 3). Thus, phosvitin is converted largely to an ordered β-sheet conformation at pH (or pD) 1.5. The magnitudes of the frequency and intensity shifts in the Raman spectra of phosvitin accompanying the pH- and pD-induced structure transitions are demonstrated by the difference spectra of Figure 4.

Deconvolution and Curve-Fitting Methods Indicate a Large Increase of Phosvitin β-Sheet Structure at Low pH. To provide a semiquantitative indication of the change in phosvitin secondary structure, we have decomposed the Raman amide I profile using both Fourier deconvolution and curve-fitting methods. The relative abundance of a given conformer is estimated from the relative integrated intensity of its corresponding band component, after deconvolution (Thomas & Agard, 1984) or curve fitting (Williams, 1983).

The deconvolution results are shown in Figure 5. Three components to amide I are suggested by deconvolution of the pH 7.4 spectrum. The most intense band component, accounting for 53% of the total amide I intensity, occurs at 1687 cm^{-1} and is ascribed to the unusual backbone conformation noted above. The component of intermediate intensity (36%) at 1664 cm^{-1} could be due to either disordered or β-sheet structure. The weakest component (11%) at 1650 cm^{-1} coincides with α-helix structure (Chen & Lord, 1974). By comparison, at pH 1.5, the deconvoluted amide I bands and their relative intensities are 1674 (72% β-sheet) and 1648 cm^{-1} (28% α-helix). A strict quantitative interpretation of these results would depend upon a definitive assignment of the 1664-cm^{-1} band component to either sheet or disordered structure in the pH 7.4 spectrum. Since this is not possible, we define instead two limiting interpretations of the data. In the more conservative alternative (listed in Table II), which assumes no disordered structure at pH 7.4, the β-sheet structure would be increased from 36% at pH 7.4 to 72% at pH 1.5. Conversely, if we assume no β-sheet structure at pH 7.4, then the net increase in β-sheet is from 0 to 72%. It is not possible to decide between these interpretations on the basis of the deconvolution results alone.

Table II: Estimation of Phosvitin Secondary Structure by Fourier Deconvolution of Raman Amide I and I′ Bands[a]

conditions	% strand	% helical	% other
pH 7.4	35.5[b]	11.5	53.0
pD 7.5	35.0[b]	*c*	*c*
pH 1.5	72.0	28.0	
pD 1.5	85.0	15.0	

[a] Each entry is reproducible to ±5%, for a wide range of deblurring functions. See Thomas and Agard (1984). The estimated error in each entry, resulting from noise inherent in the spectra, is ±10% of the value listed. [b] Disordered regions not measured separately from β-sheet structure. [c] Bands not resolved. See Figure 5.

The small increase in α-helix structure (from 11.5 to 28%) suggested by the deconvolution intensity near 1650 cm^{-1} is regarded as marginal, in view of the effects of interference from liquid water near this frequency. The deconvolution of the amide I′ band of the corresponding D_2O solution spectra confirms the large increase in β-structure with little or no change in α-helix structure accompanying the pD-induced transition (Table II).

The reference library for curve fitting the phosvitin amide I profile was provided by Dr. R. W. Williams. It consists of amide I bands obtained from 16 proteins of known three-dimensional structure and representative of a number of different secondary structure types (Williams, 1983). However, the

library does not contain any protein with an amide I band as high in frequency as that of neutral phosvitin (1682 cm^{-1}). Therefore, the fit of the pH 7.4 phosvitin spectrum is poor, and meaningful results cannot be obtained on the neutral form of the protein by this curve-fitting procedure. On the other hand, the amide I band of phosvitin at acidic pH is fit to within 5% residuals by the following four-state model: 14% disordered, 14% helix, 48% sheet, and 15% turn. Thus, by both curve fitting and deconvolution the predominant type of structure for the pH 1.5 form of phosvitin is β-sheet. Since the deconvolution method does not separately distinguish β-turns from other structure types, the two methods are actually in reasonably good agreement with one another.

Protein Secondary Structure Predictions Confirm Low Percentages of Ordered Structure in Phosvitin. Programs for prediction of protein secondary structure (Finer-Moore et al., 1984), adapted from the original work of Chou and Fasman (1978) and Robson and co-workers (Garnier et al., 1978), have also been applied to phosvitin. Although these algorithms are incapable of dealing rigorously with the phosphorylated serine residues, they do provide an indication that the anomalous Raman amide I frequency (1682 cm^{-1}) of the pH 7.4 form of the protein is not due to an ordered structure of the β-sheet or α-helix type. Using serine in place of phosphoserine throughout the phosvitin sequence, we obtained by both methods 20% or less ordered structure (i.e., α-helix plus β-sheet) in phosvitin. The Robson method yields 11% helix, 2% sheet, 64% disordered, and 23% turn. The Chou–Fasman prediction is 13% helix, 7% sheet, 10% disordered, and 70% turn.

Comparison with Model Compounds Provides No Evidence for Extensive β-Turns in Phosvitin. The Chou–Fasman prediction described in the preceding section implies that turns could be an important structural component of phosvitin. In order to further evaluate whether β-turns may be the source of the strong 1682-cm^{-1} Raman line (resolved at 1687 cm^{-1} by deconvolution), we have compared the present spectra with available Raman data from model compounds representative of β-turn conformations. Specifically, we have examined Raman data from the following: (i) several cyclic peptides characterized by NMR spectroscopy as containing β-turns (Seaton, 1983), (ii) the cyclopentadecapeptide $(VPGVG)_3$, known from X-ray crystallography to form β-turns (D. W. Urry and G. J. Thomas, Jr., unpublished results), and (iii) the polypentapeptide poly(VPGVG), known from NMR studies to form extensive β-turns (D. W. Urry and G. J. Thomas, Jr., unpublished results). None of the compounds investigated exhibits a strong Raman line near 1682 cm^{-1}. As noted above, the calculated normal modes of vibration of several types of β-turns provide no evidence for both an amide I Raman component near 1680–1685 cm^{-1} and an amide III component near 1250–1260 cm^{-1} (Krimm & Bandekar, 1980; Lagant et al., 1984a,b). We therefore consider it unlikely that the unusual structure of phosvitin consists substantially of β-turns.

Side Chains of Phosvitin Remain Significantly Ionized at Low pH. Since phosphoserines account for approximately 55% of the amino acids, many of the prominent lines in the spectra can be assigned to vibrations of these residues. The lines at 1085 and 977 cm^{-1}, which are the two most intense in the pH 7.4 spectrum, are due to symmetrical PO stretching vibrations of $C-O-P(OH)O_2^-$ and $C-O-PO_3^{2-}$ groups, respectively (Thomas & Hartman, 1973). The relative intensities of the two lines in the Figure 1 spectrum show that at these conditions the equilibrium lies in favor of a somewhat greater concentration of the monoanionic form. In the pD 7.5 spectrum (Figure 2), on the other hand, the concentration of dianionic species prevails slightly. It is not clear whether the marginally different relative intensities observed for H_2O and D_2O solutions are due to the slightly different acidities (pH 7.4 vs. pD 7.5) or to an isotope effect upon the equilibrium governing the secondary dissociation of the phosphomonoester group or to both of these factors. It is clear, however, that at pH 1.5, with the disappearance of the 977-cm^{-1} line, the concentration of dianionic species is negligible.

The same is true of the low-pD solution. The Raman line at 985 cm^{-1} in the pD 1.5 spectrum (Figure 2) is due to the amide III′ mode of β-sheet structure, as noted earlier, and not to dianionic phosphate. These results show that Raman spectroscopy would provide a convenient method for quantitative assessment of the state of ionization of phosphoserine groups in phosphorylated proteins.

The strong line at 844 cm^{-1} in the pH 7.4 spectrum is shifted slightly to higher frequency (849 cm^{-1}) and also gains intensity at low pH (Figure 1). Similar changes are observed for the 834-cm^{-1} line of deuterated phosvitin (Figure 2). The absence of a corresponding Raman line in poly(L-serine) (Figure 3) shows that the frequency does not originate from serine itself but from the phosphorylated serine residue. We assign the frequency to a quasi-symmetrical OPO stretching vibration of the C–O–P–O–H network in the monoanionic form of phosphoserine. It is interesting to note the near coincidence of this frequency with a similar phosphodiester group vibration of nucleic acid backbones, especially that of B DNA (Prescott et al., 1984).

The Raman lines of phenylalanine, tyrosine, and tryptophan, normally prominent in protein spectra, are difficult to detect in phosvitin because of interference from phosphoserine groups. Conversely, the imidazole ring vibrations of histidine, generally weak or undetected in spectra of globular proteins, are promoted to prominence in phosvitin because of the relative abundance of this amino acid. A recently established correlation between the intensity of the histidyl ring mode near 1408 cm^{-1} and the ionization state of the imidazole ring may be applied to phosvitin (Harada et al., 1982). Thus, the prominent line at 1406 cm^{-1} in the pD 1.5 spectrum (Figure 2) may be taken as the reference intensity for fully deuteronated imidazolium rings of phosvitin. The apparent retention of most (or all) of this intensity at pD 7.5 indicates that the imidazolium rings remain ionized at slightly above neutral pD. This represents a significant departure from the behavior noted for imidazolium ionization in ribonuclease (Harada et al., 1982) and suggests a substantial upward shift in the pK (normally 5.9 in L-histidine) governing dissociation of the imidazolium ion.

This interpretation is supported by the spectra of H_2O solutions of phosvitin. A band at 1629 cm^{-1}, characteristic of the positively charged imidazolium ion (Ashikawa & Itoh, 1979) and observed as a shoulder in the pH 1.5 spectrum, is substantially conserved in the pH 7.4 spectrum. The band is clearly resolved at 1627 cm^{-1} by deconvolution in Figure 5. The present findings are consistent with the results of pH titration studies of imidazoles of phosvitin, monitored by ^1H NMR spectra, which show the pK value of the histidine side chain to be around 7.45 (Vogel, 1983). A likely cause of the difficulty in abstraction of imidazolium protons of phosvitin is interaction with negatively charged phosphoserine groups.

Phosvitin Assumes the β-Sheet Conformation in the Solid State. Figure 6 shows the Raman spectrum of phosvitin in the solid state. The solid was lyophilized from a *neutral* solution, which originally yielded the same spectrum shown

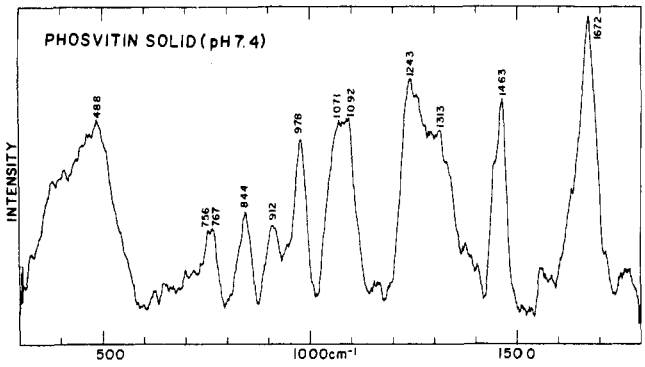

FIGURE 6: Raman spectrum of solid phosvitin, lyophilized from H_2O solution at pH 7.4.

in Figure 1 (pH 7.4). The conservation of neutrality with lyophilization is confirmed by the fact that the general pattern of 978- and 1092-cm^{-1} lines in the solid-state spectrum agrees closely with the 977- and 1085-cm^{-1} pattern observed in the neutral-solution spectrum but not with the pattern of the acidic-solution spectrum (cf. Figure 6 with Figure 1). Thus, the state of ionization of phosphoserines (and evidently other side chains as well) has not been significantly altered by the change of state of aggregation of the protein from neutral aqueous solution to neutral solid. Yet, remarkably, the amide I and III bands of phosvitin have changed greatly. *With lyophilization the amide I and III bands assume the pattern observed for the β-sheet structure of low-pH phosvitin, even though the effective pH has remained constant as judged by phosphoserine side-chain ionizations.* These results suggest that condensation alone produces a structure transition of phosvitin to the β-sheet conformation.

Conclusions

We conclude from the present studies that the majority of peptide groups in the protein chain of phosvitin adopt an unusual conformation at physiological pH (or pD). This structure may be characterized as containing (i) very little α-helix conformation, (ii) a minority of residues in β-sheet and/or irregular conformations, and (iii) a majority of residues in an unusual, heretofore undetected, conformation. The structure at physiological pH is also not likely to be rich in β-turns. Although, geometric details of the structure cannot be determined from the spectra, the Raman amide bands of phosvitin indicate that the dominant conformation is one that has not been encountered previously in globular proteins and model polypeptides.

Quantitative estimation of secondary structure by application of deconvolution methods to the experimental data indicates that 65% or more of the protein chain is not involved in helix or sheet domains. Protein secondary structure prediction methods confirm the low probability of ordered-helix and sheet structures in the phosvitin sequence. The Robson method predicts that 65% of the protein does not comprise conventional helix, sheet, and turn conformations, in good agreement with the experimental results.

Removal of the aqueous solvent by lyophilization of phosvitin from neutral solution produces, as expected, little or no change in the states of ionization of phosphoserines but, surprisingly, produces a large-scale change to conventional β-sheet secondary structure. The same secondary structure transition of phosvitin is achieved by reduction of the solution pH (pD) to 1.5. The β-sheet structure characteristic of the low-pH and solid-state forms of phosvitin is virtually indistinguishable by Raman spectroscopy from the β-sheet structure of poly(L-serine). As much as 72% β-sheet structure is indicated by deconvolution of the amide I Raman band of low-pH phosvitin. The deconvolution result may be an overestimate, however, because strand and disordered segments are not distinguished separately by this method. Nevertheless, a consistent quantitative estimate is obtained by curve fitting, which measures β-sheet (48%) and β-turn (15%) compositions separately.

Other features of phosvitin structure at physiological pH that emerge from the Raman spectra are the following: The phosphoserine side chains exist in roughly equal numbers of monoanions [C–O–P(OH)O_2^-] and dianions (C–O–PO_3^{2-}) at pH 7.4 (or pD 7.5). The imidazolium rings of histidines are also largely ionized at this pH (pD).

The present results can be explained by a model for phosvitin in which the highly negatively charged phosphoserines are only partially neutralized at physiological pH by basic protein groups, i.e., histidyl, lysyl, and arginyl side chains. Considerable repulsion between phosphate anions, especially in contiguous stretches of phosphoserines, may prevent the formation of an ordered or compact structure accessible to other proteins. Attenuation of the electrostatic repulsion, and stabilization of an ordered β-sheet structure, is evidently accomplished by lowering the solution pH. Apparently, the same effect is also achieved by lyophilization of the protein from neutral aqueous solution. Lyophilization may facilitate the retention of metal cations and water molecules in specific association with serine phosphates to reduce electrostatic repulsions.

The results obtained here may also provide an explanation for the sometimes conflicting reports on phosvitin secondary structure with different experimental techniques. We suggest that methods that probe condensed samples, including films, are likely to indicate a secondary structure that is relatively rich in β-sheet conformation, while methods that investigate true solutions, especially low-concentration solutions, are likely to provide evidence for a very different (perhaps unorthodox) protein chain conformation that is relatively deficient in β-sheet conformation.

Acknowledgments

We thank Dr. George Taborsky, University of California, Santa Barbara, for purified samples of phosvitin and for illuminating discussions on the protein structure.

Registry No. D_2, 7782-39-0; poly(L-serine), 25821-52-7; phosphoserine, 407-41-0; L-histidine, 71-00-1.

References

Ashikawa, L., & Itoh, K. (1979) *Biopolymers 18*, 1859–1876.
Byrne, B. M., van het Schip, A. D., van de Klundert, J. A. M., Arnberg, A. C., Gruber, M., & Geert, A. B. (1984) *Biochemistry 23*, 4275–4279.
Chen, M. C., & Lord, R. C. (1974) *J. Am. Chem. Soc. 96*, 4750–4752.
Chou, P. Y., & Fasman, G. (1978) *Adv. Enzymol. 47*, 45–148.
Clark, R. C. (1970) *Biochem. J. 118*, 537–542.
Finer-Moore, J., Stroud, R. M., Prescott, B., & Thomas, G. J., Jr. (1984) *J. Biomol. Struct. Dyn. 2*, 93–100.
Garnier, J., Osguthorpe, D. J., & Robson, B. (1978) *J. Mol. Biol. 120*, 97–120.
Harada, I., Takamatsu, T., Tasumi, M., & Lord, R. C. (1982) *Biochemistry 21*, 3674–3677.
Joubert, F. J., & Cook, W. H. (1958) *Can. J. Biochem. Physiol. 36*, 399–408.
Krimm, S., & Bandekar, J. (1980) *Biopolymers 19*, 1–29.
Lagant, P., Vergoten, G., Fleury, G., & Loucheux-Lefebvre, M.-H. (1984a) *Eur. J. Biochem. 139*, 137–148.

Lagant, P., Vergoten, G., Fleury, G., & Loucheux-Lefebvre, M.-H. (1984b) *Eur. J. Biochem. 139*, 149–154.
Li, Y., Thomas, G. J., Jr., Fuller, M., & King, J. (1981) *Prog. Clin. Biol. Res. 64*, 271–283.
Lord, R. C., & Thomas, G. J., Jr. (1967) *Spectrochim. Acta, Part A 23A*, 2551–2591.
Perlmann, G. E., & Grizzuti, K. (1971) *Biochemistry 10*, 258–264.
Prescott, B., Steinmetz, W., & Thomas, G. J., Jr. (1984) *Biopolymers 23*, 235–256.
Renugopalakrishnan, V., Horowitz, P. M., & Glimcher, M. J. (1985) *J. Biol. Chem. 260*, 11406–11413.
Seaton, B. (1983) Ph.D. Thesis, Department of Chemistry, Massachusetts Institute of Technology.
Shainkin, R., & Perlmann, G. E. (1971) *Arch. Biochem. Biophys. 145*, 693–700.
Taborsky, G. (1970) *J. Biol. Chem. 245*, 1054–1062.
Thomas, G. J., Jr. (1985) *Spectrochim. Acta, Part A 41A*, 217–221.
Thomas, G. J., Jr., & Hartman, K. A. (1973) *Biochim. Biophys. Acta 312*, 311–322.
Thomas, G. J., Jr., & Agard, D. A. (1984) *Biophys. J. 46*, 763–768.
Thomas, G. J., Jr., Prescott, B., & Day, L. A. (1983) *J. Mol. Biol. 165*, 321–356.
Timasheff, S. N., Townend, R., & Perlmann, G. E. (1967) *J. Biol. Chem. 242*, 2290–2292.
Verduin, B. J. M., Prescott, B., & Thomas, G. J., Jr. (1984) *Biochemistry 23*, 4301–4308.
Vogel, H. J. (1983) *Biochemistry 22*, 668–674.
Williams, R. W. (1983) *J. Mol. Biol. 166*, 581–603.
Williams, R. W., Dunker, A. K., & Peticolas, W. L. (1984) *Biochim. Biophys. Acta 791*, 131–144.

Resonance Raman Study on Proton-Dissociated State of Bacteriorhodopsin: Stabilization of L-like Intermediate Having the All-Trans Chromophore†

Akio Maeda*
Department of Biophysics, Faculty of Science, Kyoto University, Kyoto 606, Japan
Takashi Ogura and Teizo Kitagawa*
Institute for Molecular Science, Okazaki National Institute, Okazaki 444, Japan
Received June 12, 1985; Revised Manuscript Received November 4, 1985

ABSTRACT: The resonance Raman spectra of light-adapted bacteriorhodopsin in purple membrane were investigated in the alkaline pH region where its Schiff base was kept protonated. Upon raising the pH from 7.0 to 10.5, the spectrum of bacteriorhodopsin excited at 514.5 nm remains essentially unaltered when laser power is low, but distinct features appear due to the formation of a long-lived intermediate as the laser power is raised. The spectral characteristics of the long-lived intermediate are as follows: (1) a small shift or disappearance of the N–H (or N–D) bending mode of the protonated Schiff base, (2) the appearance of new bands at 1188 and 1159 cm^{-1}, and (3) the disappearance of the 1456-cm^{-1} line accompanied with the appearance of several bands at 1470, 1446, and 1397 cm^{-1}. The resultant resonance Raman spectrum resembled that of the L_{543} intermediate, except for the C—C, C=C, and C=N stretching frequencies, which are the same as those of bacteriorhodopsin having the all-trans chromophore. Such an L-like intermediate appears with a midpoint pH of conversion around 9 in parallel to the absorbance change at 296 nm. The pH difference spectrum of bacteriorhodopsin in the UV region was close to the alkaline – neutral difference spectrum of free tryptophan due to the ionization of an amino acid residue in the vicinity of tryptophan. The residue responsible for the ionization at pH 9 is tentatively assigned to the carboxylate with an unusually high pK_a, as pointed out by Engelhard et al. [Engelhard, B., Gerwert, K., Hess, B., Kreutz, W., & Siebert, F. (1985) *Biochemistry 24*, 400]. It is stressed that its ionization stabilizes the L-like intermediate having the all-trans chromophore.

Bacteriorhodopsin (bR)[1] is the only protein in the purple membrane, which is formed as a differentiated patch in the membrane of halophilic bacteria. Retinal is attached to the specific lysine residue of the protein through the protonated Schiff base. The bR molecule possessing *all-trans*-retinal conveys two protons unidirectionally for each photocycle [see the review by Stoeckenius & Bogomolni (1982)] containing several intermediates called K_{610}, KL_{590}, L_{543}, M_{412}, and O_{640} in order of their appearance (Stoeckenius et al., 1979; Shichida et al., 1983). These intermediates are characterized by their visible absorption and resonance Raman (RR) spectra (Marcus & Lewis, 1978; Terner et al., 1979; Braiman & Mathies, 1980, 1982; Argade & Rothschild, 1983; Smith et al., 1983, 1984; Alshuth & Stockburger, 1986). The light energy once stored in the 13-cis isomer of the retinal chromophore is transmitted to the protein moiety to translocate protons. The structural mechanism for the proton transfer has been a subject of recent spectroscopic studies.

† This work was supported by the Grant-in-Aids for Special Project Research on Molecular Mechanism of Bioelectrical Response to A.M. (59123002) and T.K. (59223015) from the Japanese Ministry of Education, Science and Culture. This work was also supported by the Joint Studies Program (1985) of the Institute fo. Molecular Science (Okazaki, Japan).

[1] Abbreviations: bR, bacteriorhodopsin; RR, resonance Raman; FTIR, Fourier transform infrared; λ_{max}, wavelength for maximum absorption.

0006-2960/86/0425-2798$01.50/0